Voltammetric Probes of Cytochrome Electroreactivity: The Effect of the Protein Matrix on Outer-Sphere Reorganization Energy and Electronic Coupling Probed through Comparisons with the Behavior of Porphyrin Complexes†

Jeffrey I. Blankman,‡,§ Nazim Shahzad,|| Bindi Dangi,|| Cary J. Miller,*,⊥ and R. D. Guiles*,||

Department of Chemistry and Biochemistry, University of Maryland, College Park, Maryland 20742, and Department of Pharmaceutical Sciences, University of Maryland, Baltimore, Maryland 21201

Received March 31, 2000; Revised Manuscript Received August 24, 2000

ABSTRACT: Using surface-modified electrodes composed of ω-hydroxyalkanethiols, an experimentally based value for the inner-sphere reorganization energy of the bis(imidazole)iron porphyrin system has been obtained by examining the solvent dependence of the reorganization energy of bis(*N*-methylimidazole)-*meso*-tetraphenyl iron porphyrin. The value obtained (0.41 ± 0.06 eV) is remarkably similar to values we have recently reported for the reorganization energy of cytochrome b_5 (0.43 ± 0.02 eV) and cytochrome *c* (0.58 ± 0.06 eV). This strongly suggests that the protein matrix mimics the behavior of a low dielectric solvent and effectively shields the heme from the solvent. The effect of the orientation of the heme relative to the electrode was also explored by sytematically varying the steric bulk of the axial ligands. On the basis of a good linear correlation between the electronic coupling and the cosine of the angle between the heme plane and the surface of the electrode, it is suggested that a parallel orientation of the heme yields a maximum in the electronic coupling. Relevance to interheme protein electron transfer is discussed.

According to Marcus theory, the facility of electron transfer is dictated dominantly by two terms: the reorganization energy and the electronic coupling between redox active centers (*1*, *2*). The role of the protein matrix and/or the solvent in contributing to the outer-sphere component of the reorganization energy in cytochromes has been a major focus of debate (*3*−*5*). Similarly, the protein's role in mediating electronic coupling has been a major focus of research efforts (*3*−*8*).

We have previously shown that the use of surface-modified electrodes employing self-assembling monolayers composed of ω-hydroxyalkanethiols in direct voltammetric measurements of heme proteins can reliably yield accurate values for these Marcusian kinetic parameters (*9*−*11*). In this paper, we explore the contribution of the protein and/or solvent to the reorganization energy by comparisons to reorganization energies determined for a series of porphyrin complexes. Our approach involves an experimentally based determination of the reorganization energy for the bis(imidazole) porphyrin system through an analysis of the solvent dependence of the reorganization energy. From this inner-sphere term, the outer-sphere contribution of the reorganization energy for cytochromes b_5 and *c* can be estimated.

Although the partitioning of the reorganization energy into inner- and outer-sphere components is in principle somewhat arbitrary and a subject of debate for heme proteins (*1*, *3*, *4*), theoretical methods for calculating these two components were developed by Marcus and have served as a useful model in the description of the behavior of a number of systems (*1*, *5*, *12*). The total reorganization energy, λ, is taken to be the sum of these two terms (*1*, *13*):

$$\lambda = \lambda_{is} + \lambda_{os} \tag{1}$$

where λ_{is} is the inner-sphere reorganization energy and λ_{os} is the outer-sphere component.

The inner-sphere term is taken to be the sum of the squares of all inner-sphere bond length changes associated with the oxidation state change weighted by a force constant associated with the specific bonds:

$$\lambda_{is} = \sum_i k_i \Delta l_i^2 \tag{2}$$

The outer-sphere term is determined by the energy necessary to charge the dielectric medium surrounding the inner sphere, given by

$$\lambda_{os} = 6.24 \times 10^{18} \frac{n^2 e^2}{8\pi\epsilon_o r}\left[\frac{1}{\epsilon_{op}} - \frac{1}{\epsilon_s}\right] \tag{3}$$

where ϵ_{op} and ϵ_s are the optical and static dielectric constants, *r* is the radius of the inner sphere, *n* is the number of electrons transferred, *e* is the charge of the electron in coulombs, and ϵ_o is the electric permittivity. The affect of the image charge has been ignored in this form of the equation (*13*).

† The generous support of the National Science Foundation (CHE 9417357 to C.J.M. and MCB 9904422 to R.D.G.) is gratefully acknowledged.

* To whom correspondence should be addressed.

‡ Department of Chemistry and Biochemistry.

§ Current address: Wyeth-Ayerst ESI Lederle, 2 Easterbrook Lane, Cherry Hill, NJ 08003.

|| Department of Pharmaceutical Sciences.

⊥ Current address: i-Stat Corporation, 436 Hazeldean, Kanata, Canada K2L 1T9.

10.1021/bi0007324 CCC: $19.00
Published on Web 11/02/2000

The term in square brackets is referred to as the Pekar factor. In measuring the reorganization energy for bis(*N*-methylimidazole)tetraphenyl iron porphyrins in a series of solvents spanning a range of Pekar factors, it is possible to extrapolate to zero Pekar factor, yielding an experimentally based estimate of the inner-sphere term for the bis(imidazole) porphyrin system. Our recent characterizations of the Marcus theory kinetic parameters for cytochromes b_5 (*10*, *11*) and *c* (*9*, *11*) using identical experimental and theoretical procedures enable realistic comparisons with the results obtained with the porphyrin model systems.

The ability to compare reorganization energies of porphyrin systems in different solvents and to the behavior in a protein is due to the fact that this term is determined from fits to the functional form of the current at overpotentials measured relative to the reduction potential and hence is not prone to the difficulties in comparing absolute reduction potentials in different solvents due to junction potential effects (*14*, *15*).

The affect of the orientation of the porphyrin relative to the electrode in heme systems has also been explored by systematically varying the steric bulk of the axial ligands. Comparisons of measured electronic coupling magnitudes measured for cytochrome b_5 suggest that the edge on approach of the heme forced by the protein matrix is not the optimum coupling geometry and accounts for much of the reduced magnitude in the observed current relative to the models.

Bis(imidazole) and bis(pyridine) porphyrin complexes have been characterized extensively structurally, spectroscopically, and electrochemically (*16*−*18*). Previous electrochemical characterizations have focused on thermodynamic properties of the porphyrin complexes such as reduction potentials as a function of the characteristics of the axial ligands and axial ligand exchange kinetics (*16*). Such studies have led to a greater understanding of factors dictating electronic structure of cytochromes and factors which control differences in reduction potentials in this class of proteins. This paper explores the use of model systems in the elucidation of important factors controlling the kinetics of electron transfer. The relevance to an understanding of long-range interheme protein electron transfer is discussed.

EXPERIMENTAL SECTION

Cytochrome Preparation. The rat cytochrome b_5 was overexpressed in *Escherichia coli* using a synthetic gene construct (*19*) employing a pET3c vector as previously described (*20*). Electrochemical measurements of the cytochrome were performed in 0.96 M KCl and 2 mM phosphate buffer (pH 7.1). Commercially available cytochrome *c* (Sigma) was used without further purification. Solution conditions were identical to those of cytochrome b_5.

FeTPP(NMe-Im)$_2$ Synthesis. The tetraphenyl iron porphyrin used in this paper was synthesized using a minor modification of the published procedure (*18*). The iron porphyrin was purified using silica gel column chromatography. The free porphyrin was eluted with methylene chloride until no color was apparent in the eluent. The iron porphyrin was eluted with a 10% methanol/methylene chloride solution. The resulting solution was evaporated, and the solid was dissolved in *N*-methylimidazole (Sigma) and allowed to equilibrate overnight. The solution was evaporated to dryness, and the solid was collected and used immediately.

FeTPPS(L)$_2$ Synthesis. The water-soluble iron porphyrins studied in this paper were prepared using minor modifications of published procedures (*21*−*23*). Typical yields for these reactions were approximately 85% relative to the porphyrin starting material as measured by coulometry in a calibrated thin layer cell.

Bis(pyridine) ligation of the iron in the reduced state of the porphyrin complex was confirmed through a comparison of the NMR spectra of the Fe(II) porphyrin and a Zn(II) analogue which exhibited nearly identical NMR spectra confirming a low-spin diamagnetic d^6 ground state. Assignment of pyridine proton NMR resonances was confirmed using deuterated ligands. All proton NMR measurements were performed using a General Electric QE-300 MHz NMR spectrometer. In addition, the ligation state of the porphyrin complexes was verified electrochemically by monitoring the peak potentials in the presence of various amounts of the axial ligand. No shifts in the voltammetric potentials were observed suggesting complete coordination of the pyridyl ligands at the two axial positions of the complex.

Aqueous Electrochemical Measurements. The ω-hydroxyalkanethiols were synthesized, purified, and adsorbed onto freshly sputtered and cleaned Au electrodes (0.13 cm^2 active area) as described previously (*14*). All electrochemical experiments were performed in a jacketed electrochemical cell held at 0.0 °C, utilizing a Bioanalytical Systems BAS-100A or BAS-100B Electrochemical Analyzer. A standard three-electrode cell was used with a Pt counter electrode, and all measurements are reported versus a saturated calomel reference electrode (SCE).[1] All solutions were held under a N_2 atmosphere during the electrochemical experiments. The redox concentration of each solution was determined by coulometric assay in a calibrated thin layer cell prior to kinetic experiments. Solutions of the *meso*-tetrakis(sulfonatophenyl)porphyrins for electrochemical analysis were prepared by dissolving a known quantity of the solid in 0.25 M KCl.

Nonaqueous Electrochemical Measurements. All nonaqueous electrochemical experiments were performed in dry solvents: methylene chloride, dimethyl formamide, dimethyl sulfoxide, chloroform, tetrahydrofuran, and acetonitrile, with 1.5 M *tert*-butylammonium perchlorate as the supporting electrolyte. All electrochemical measurements were performed at 0 °C under a nitrogen blanket with a saturated calomel reference electrode. The reference electrode was soaked in deionized water for several minutes prior to immersion in the solvent to minimize chloride leakage.

Molecular Modeling of Porphyrin Structures. The porphyrin complex structures were model built using the program MacSpartan (*24*). The geometries were optimized using a semiempirical approach employing PM3 parameters. Generally, bond lengths are found to agree with experimentally determined values to within 0.03 Å (*24*). Because of the rigid planar nature of the porphyrin macrocycle and the

[1] Abbreviations: DMF, dimethyl formamide; DMSO, dimethyl sulfoxide; DOCA, distance of closest approach; NMe-Im, *N*-methyl imidazole; PZC, potential of zero charge; SCE, saturated calomel electrode; TPP, *meso*-tetraphenyl porphyrin; TPPS, *meso*-tetrakis(4-sulfonatophenyl)porphyrin.

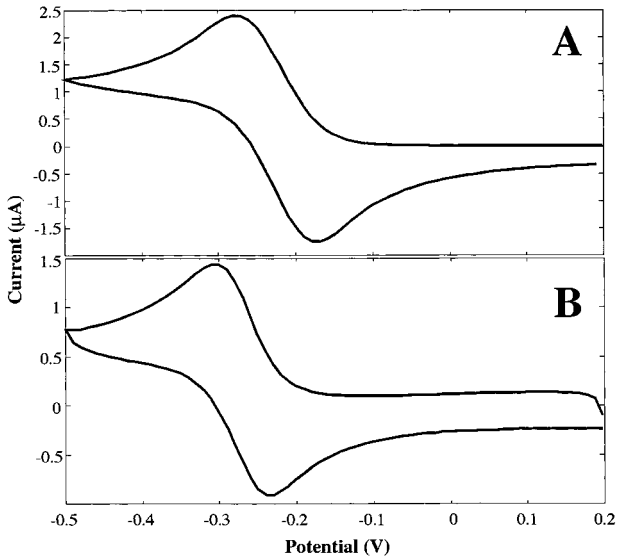

FIGURE 1: Cyclic voltammogram of (A) 3.0 mM cytochrome b_5 in 0.96 M KCl and (B) 1.0 mM FeTPPS(*N*-methylimidazole)$_2$ in 0.25 M KCl on gold electrodes modified with 3-mercaptopropanol. The cytochrome b_5 experiments were performed in 2 mM, pH 7.1, phosphate buffer at 50 mV/s. The temperature of the cell was held at 0.0 °C. Potentials were recorded and are reported versus the saturated calomel electrode (SCE). The electrode areas were 0.13 cm^2.

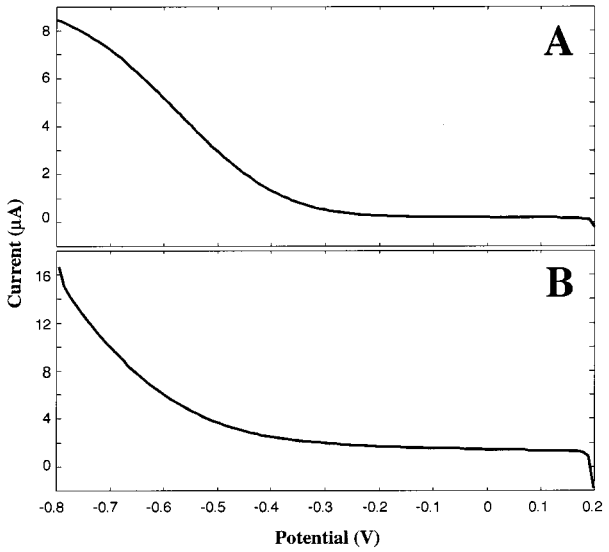

FIGURE 2: Cyclic voltammogram of the solutions described in Figure 1 using gold electrodes modified with 11-mercaptoundecanol and 14-mercaptotetradecanol, respectively. Scan rate (A) 0.5 V/s and (B) 5.12 V/s. The electrode area was 0.13 cm^2. Potentials were recorded and are reported versus the saturated calomel electrode. The protein voltammogram was obtained in 2 mM, pH 7.1, phosphate buffer. Temperatures were held at 0.0 °C.

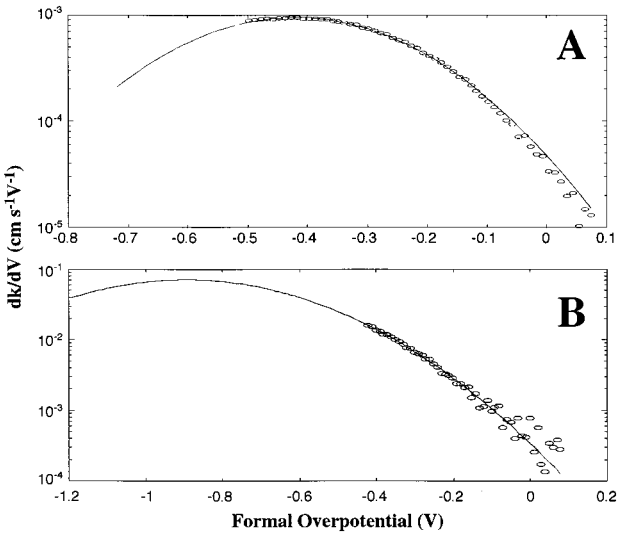

FIGURE 3: Plots of the potential derivative of the heterogeneous electron-transfer rate constant for the heme proteins derived from the data shown in Figure 2. These derivative plots are proportional to the density of electronic states distributions of the redox species at the monolayer coated electrode surface. The labels (A and B) correspond to cytochrome b_5 and FeTPPS(*N*-methylimidazole)$_2$, respectively. The solid curves represent the best fit Gaussian to the experimental points.

axial ligands, bond angles are also in good agrreement (i.e., within a few degrees of experimentally observed values). These error limits are verifiable for two of the complexes used in this study in that X-ray crystal structures are known for bis(pyridine)iron tetraphenylporphyrin (*25*) and bis(*N*-methylimidazole)iron tetraphenylporphyrin (*26*). In addition the structure of of bis(imidazole)iron tetraphenylporphyrin is also known (*27*). Given the nature of substituents employed in the homologous series of complexes studies it is not expected that steric effects would cause significant deviations from the structures of the porphyrin cores. Two sources of distortion from planarity, generally in the form of S_4 ruffling, have been noted for the porphyrin macrocycle in complexes involving; axial ligands with electron withdrawing substituents (*17*, *28*) and a high degree of steric inteaction between bulky meso substituents and axial ligands (*17*). It should also be noted that the parameters derived from the modeled structures, the distance of closest approach of the Fe to the electrode surface and the angle of the porphyrin plane, are not particularly sensitive to small differences between modeled and expermentally determined structures. Angles between the plane of the porphyrin ring and the electrode surface were determined from the arcsine of the ratio of the normal distance of closest approach of the iron to the electrode surface and the distance from the iron to the electrode surface along the plane of the porphyrin, usually defined by one of the meso carbons. The electrode surface was modeled as a planar array of points as shown in Figure 5.

RESULTS

Insulating Au electrodes with short ω-hydroxyalkanethiol monolayers permit direct voltammetric investigation of the cytochromes in sharp contrast to the apparent lack of electroactivity seen at unmodified electrodes (*29*). The ω-hydroxyalkanethiol monolayers' ability to protect the gold surface from passivation by the proteins is dependent upon the formation of a uniform hydrophilic surface. We have seen that incomplete monolayers, and monolayers with hydrophobic termination, passivate quickly upon exposure to protein solutions. Nearly reversible voltammetry is observed for cytochrome b_5 at electrodes coated with HO-$(CH_2)_3$SH as is shown in Figure 1. The bare electrode responses in the same solutions give voltammetric currents which lack discernible faradaic currents relative to the background currents. The voltammogram of the cytochrome is remarkably similar to voltammograms of the bis(imidazole) porphyrin complexes as is illustrated by the voltammogram

Table 1: Formal Potential, Diffusion Coefficient, Distance of Closest Approach, Effective Charge, and Angle of the Heme at Closest Approach

species or axial ligand	formal potential (V vs SCE)	D_o[a] ($\times 10^6$ cm^2/s)	DOCA[b] (Å)	Z_{eff}[c]	angle (ϕ)[d] (deg)
pyridine	−0.273	2.1 ± 0.6	6.5	−3	26.8
4-methylpyridine	−0.252	3.0 ± 0.8	7.1	−3	35.4
4-*tert*-butylpyridine	−0.258	2.7 ± 0.6	7.7	−3	42.2
4-phenylpyridine	−0.247	2.1 ± 0.5	8.4	−3	46.5
N-methylimidazole	−0.272	2.1 ± 0.2	6.4	−3	23.6
cytochrome *c*	0.023	0.47 ± 0.03	9.5	2.4 ± 0.3	90
cytochrome b_5	−0.213	0.38 ± 0.08	7.1	−1.4 ± 0.5	90

[a] Diffusion coefficients were determined at 0.0 °C. The reported uncertainties are standard deviations from repeated measurements. [b] The distance of closest approach of the iron center to the electrode surface was calculated by determining the normal distance between the iron and a planar array of points which were in van der Waals contact with the model compound. The analysis was performed using Midas plus on a Silicon Graphics Workstation. Geometries of porphyrin complexes were calculated using MacSpartan Plus using a semiempirical approach using PM3 parameters (*24*, *33*). X-ray crystal structures are known for two of the porphyrin complexes studied [i.e., bis(pyridine)FeTPP (*25*) and bis(*N*-methylimidazole)FeTPP (*26*)]. The small differences between calculated and crystallographically characterized structures do not affect the distances of closest approach to an uncertainty of 0.1 Å or angles of interaction to within 5°. [c] The effective charge for the protein was calculated by changing the ionic strength of the solution from 0.10 to 1.0 M at 0.0 °C and the heterogeneous electron-transfer rate constants were measured at $HO(CH_2)_{11}SH$ electrodes. The diffuse layer potential was calculated at both ionic strengths and the effective charge was determined. [d] The angle of the porphyrin with respect to the electrode surface. The cytochromes were set to be perpendicular to the electrode surface.

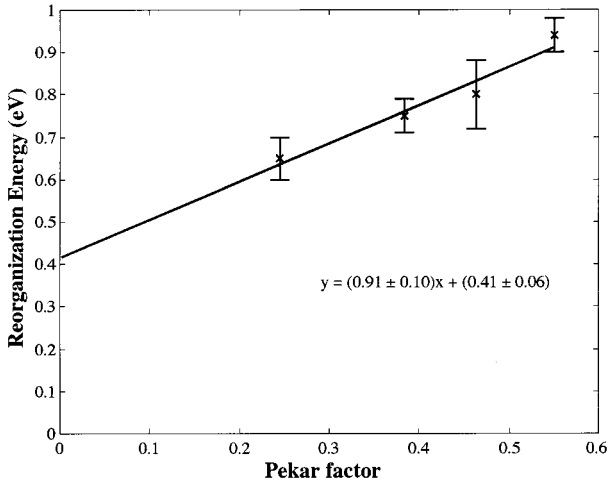

FIGURE 4: Graph of the reorganization energy of $FeTPP(Me\text{-}Im)_2$ in solvents with different Pekar factors. The best fit line is displayed with an intercept of 0.41 ± 0.06 eV. The intercept is an approximation to the inner-sphere reorganization energy.

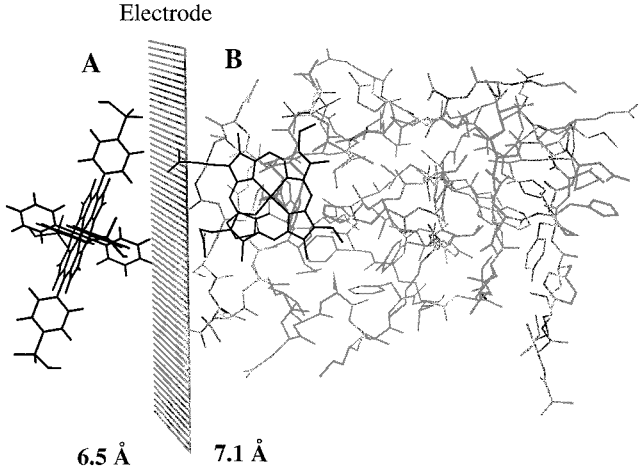

FIGURE 5: Modeled structure of the iron porphyrin system with pyridine as the axial ligands (A) and cytochrome b_5 (B) at the distance of closest approach to the electrode surface. The distance of closest approach is labeled in angstroms.

of the bis(*N*-methylimidazole) porphyrin complex shown in Figure 1B.

Reorganization Energy and Electronic Coupling Determinations. The use of ω-hydroxyalkanethiols with longer hydrocarbon chain lengths to insulate the Au electrodes allows one to measure the heterogeneous electron-transfer kinetics of small molecules and redox proteins as a function of the electrode potential. Using $HO(CH_2)_{14}SH$-coated electrodes for the porphyrin complexes, and $HO(CH_2)_{11}SH$-coated electrodes for the cytochrome b_5 and nonaqueous porphyrins, we find the heterogeneous electron transfer rates are decreased sufficiently to allow their measurement over the accessible voltammetric range of the insulated electrode. Figure 2 displays representative voltammograms for these iron porphyrins and cytochrome b_5 using longer chain length ω-hydroxyalkanethiol derivatized electrodes. Table 1 includes the formal potentials and the relevant kinetic parameters for the complexes in this study.

A unique capability of these insulated electrode studies is their ability to separate activation and electronic coupling influences on the redox molecule's redox reactivity. To obtain activation energy and electronic coupling parameters, the reduction current for the redox species is first corrected for diffusion limitations and then for electrostatic double layer effects as described previously (*14*, *30*, *31*). The corrected currents are then normalized to unit electrode area and redox concentration to give the heterogeneous electron-transfer rate constants as a function of the formal overpotential. The potential derivative of the electron-transfer rate is proportional to the density of electronic states distribution of the redox species at the electrode surface. Figure 3 shows representative density of electronic states distributions for the porphyrin complexes and for cytochrome b_5. The solid line corresponds to the best-fit Gaussian which is the predicted form of the density of electronic states distribution from the Marcus theory (*13*, *31*). The position of the peak of the density of states distributions along the overpotential axis gives a measure of the reorganization energy of the species. Given the limited accessible voltammetric range, the peak of the curve was extrapolated from the experimental data. The reorganization energies determined from these insulated electrode measurements are collected in Table 2.

These density of state distributions also yield a measure of the electronic coupling between the electrode surface and the redox site in the form of the maximum electron-transfer

Table 2: Reorganization Energies and k_{max} Values for the Porphyrin Complexes and Cytochromes b_5 and c

species or axial ligand	λ^b (eV)	$k_{max}{}^b$ (cm/s)	n^c	relative $k_{max}{}^d$
pyridine	0.93 ± 0.03	$(4.7 \pm 0.6) \times 10^{-2}$	14	2710
4-methylpyridine	0.90 ± 0.04	$(3.7 \pm 0.7) \times 10^{-2}$	14	2130
4-*tert*-butylpyridine	0.93 ± 0.02	$(2.7 \pm 0.2) \times 10^{-2}$	14	1550
4-phenylpyridine	0.90 ± 0.02	$(1.9 \pm 0.1) \times 10^{-2}$	14	1090
N-methylimidazole	0.94 ± 0.02	$(5.1 \pm 0.3) \times 10^{-2}$	14	2940
cytochrome *c*	0.58 ± 0.03	$(1.3 \pm 0.2) \times 10^{-3}$	11	2.95
cytochrome b_5	0.43 ± 0.02	$(4.4 \pm 0.2) \times 10^{-4}$	11	1

[a] The voltammetric data used for the determinations of the five iron porphyrin complexes were collected in 0.25 M KCl at a scan rate of 5.12 V/s. The data for the cytochromes were collected in 1.0 M KCl, 2 mM, pH 7.1, phosphate buffer at a scan rate of 0.5 V/s. All data were determined at 0.0 °C. [b] The reported uncertainties are standard deviations from repeated measurements. [c] *n* is the number of methylene groups in the ω-hydroxyalkanethiol coating the Au electrodes which were used for these determinations. [d] The ratio of the k_{max} parameter relative to that obtained for cytochrome b_5. Using the known distance dependence of the electron-transfer rates (2.94-fold decrease/methylene group), the k_{max} values were collected first for differences in the lengths of the monolayers used.

rate, k_{max}. This k_{max} can be obtained from the area under the density of electronic states distribution. At overpotentials much larger than the reorganization overpotential, the rate of the electron transfer to the redox molecules at the electrode surface becomes independent of the electrode potential. This activationless electron transfer rate depends primarily on the probability of electron tunneling from the Au electrode through the monolayer insulator to the redox site in solution. Additionally, the k_{max} parameter also reflects the number of reactive redox molecules within the reaction layer at the insulated electrode surface. The k_{max} values determined are listed in Table 2.

Reorganization Energy of FeTPP(NMe-Im)$_2$ in Nonaqueous Solvents. The solvent has a marked effect on the reorganization energy of a redox species, as a large portion of the reorganization energy is due to solvent electrostriction and reorientation. By changing the nature of the solvent, the inner- and outer-sphere terms of the reorganization energy can be separated. This will be discussed in detail in the next section. The measurement of the reorganization energy in nonaqueous solvents using surface modified electrodes has been previously probed with ferrocene derivatives and found to be reliable (*15*). The electronic coupling terms, however, have been seen to vary due to increased solvent penetration into the monolayer and lower monolayer breakdown voltages.

To determine which solvents are appropriate for these measurements, the monolayer breakdown voltage of the HO-$(CH_2)_{11}$SH-modified gold electrodes was determined in each solvent as the point at which significant background current is observed. Applying a large negative potential to the electrode causes a large amount of current to be observed. After these destructive experiments, the capacitance of the electrode is seen to rise significantly from the 2.1 μF/cm^2 that is typical of this length electrode. This evidence suggests that there is stripping of the monolayer from the electrode surface. The monolayer breakdown voltages, formal potential of the porphyrin and potential of zero charge of the electrodes, are collected in Table 3 for each solvent.

The reorganization energy of the FeTPP(NMe-Im)$_2$ complex was determined in methylene chloride, dimethyl sulfoxide, and *N*,*N*-dimethyl formamide. In the remaining solvents, the insulated electrodes were seen to be unstable or had breakdown voltages which were too close to the formal potential of the redox molecule and, thus, were not suitable for kinetics measurements. The reorganization energy of FeTPP(Me-Im)$_2$ in these solvents is listed in Table 3.

DISCUSSION

Reorganization Energy. The reorganization energies of cytochrome *c* (0.58 eV) and the cytochrome b_5 (0.43 eV) are very low, consistent with their role as facile mediators of electron transfer, but quite different from the water-soluble iron porphyrins. These reorganization energies can be separated into inner- and outer-sphere components corresponding to molecular and solvent activation components, respectively.

The reorganization energy of the porphyrin complexes in aqueous solution are identical, within experimental errors, with a value of 0.92 eV. Given the high degree of structural similarity between the porphyrin model complexes and the heme within the cytochromes, it is likely that these heme proteins will display a similar inner-sphere component of their reorganization energies. Below, we analyze the electron-transfer kinetic properties of cytochrome b_5 in light of this assumption.

Experimental Determination of the Inner-Sphere Reorganization Energy in Nonaqueous Solvents. To obtain an accurate estimate of the inner-sphere reorganization energy of the porphyrins, the reorganization energy should be measured in a solvent which does not contribute to the reorganization energy, i.e., λ_{os} equal to 0. The only adjustable parameter in eq 3 is the Pekar factor, $(1/\epsilon_{op} - 1/\epsilon_s)$. Since measurements in a solvent with a zero Pekar factor cannot be performed, due to the fact that these solvents are nonconductive, the reorganization energy can only be estimated. By changing the solvent and plotting the reorganization energy as a function of the Pekar factor, the inner-sphere reorganization energy can be extrapolated to a zero Pekar factor.

The reorganization energies of bis(imidazole) porphyrin complexes in the nonaqueous solvents indicated in Table 3 are plotted in Figure 4. Excellent linearity is observed, and a value of 0.41 ± 0.06 eV is calculated for a solvent with a zero Pekar factor. This result, which is an experimentally based estimate of the inner-sphere reorganization energy, is extremely close to the measured reorganization energies of the cytochrome b_5 (0.43 eV) and cytochrome *c* (0.58 eV). The fact that this number is slightly lower than those reported for the cytochromes suggests that there may be some small degree of solvent exposure of the heme and that the interior of the protein behaves like a low dielectric medium. Current models of the dielectric constant of the interior of the protein indicate that it resembles that of a normal hydrocarbon, reported values ranging from 2 to 4 (*32*). From eq 3, if the protein matrix had such a low dielectric constant and a somewhat higher refractive index than that of water, a greatly diminished outer-sphere reorganization energy would be observed, consistent with this work.

Note that there is a slight but significant difference between the reorganization energies of cytochromes b_5 and *c*. This could reflect a slightly greater solvent contribution for the

Table 3: Reorganization Energy of FeTPP(NMe-Im)$_2$ in Various Solvents, and Relevant Solvent Parameters

solvent	Pekar factor[a]	monolayer breakdown voltage[b] (mV vs SCE)	PZC[c] (mV vs SCE)	$E^{o\prime}$ (V vs SCE)	λ[d] (eV)
H_2O	0.550	−800	−50	−0.245	0.94 ± 0.02
acetonitrile	0.527	−300	NA[e]	NA[e]	NA[e]
DMF	0.463	−700	−300	−0.111	0.80 ± 0.08
methylene chloride	0.383	−600	−250	−0.166	0.75 ± 0.04
chloroform	0.270	−300	NA[e]	NA[e]	NA[e]
DMSO	0.245	−700	−300	−0.104	0.65 ± 0.05

[a] This is the $(1/\epsilon_{op} - 1/\epsilon_s)$ term of eq 3. [b] Measured as the point at which significant current is observed in a solution of 1 M *tert*-butylammonium perchlorate. [c] Measured in low ionic strength solutions. [d] Reported uncertainties are standard deviations of repeated measurements. [e] Values not measured due to low monolayer breakdown voltages.

case of cytochrome *c* where it is known that there are six internally bound water molecules (*3*). Alternatively, the differences could simply reflect an inadequacy of the bis-(*N*-methylimidazole)tetraphenyl porphyrin complexes as models for cytochrome *c*.

Electronic Coupling. Comparison between the relative electronic coupling abilities of the proteins and heme model redox molecules are less straightforward. At a simplistic level, the fact that longer thiol monolayers are required to slow the electron-transfer rate for the iron porphyrins than for the redox protein, $HO(CH_2)_{14}SH$ versus $HO(CH_2)_{11}SH$, respectively, suggests that the protein is more poorly coupled to the electrode. Because the effect of each additional methylene unit in the monolayer thickness on the electron-tunneling rate is known (*13*, *14*), we can correct the k_{max} value for the different lengths of the monolayers. Factoring in the difference in the monolayer thickness, using a tunneling decay factor (β) of 1.08/methylene unit, the k_{max} is observed to decrease by approximately a factor of 2100 for cytochrome b_5 as compared to the bis(methylpyridine) iron porphyrin complex. The methylpyridine complex was chosen for this comparison because its distance of closest approach is the same as cytochrome b_5.

The k_{max} parameters depend both on the electronic coupling between the electrode and redox molecule and on the number of reactive molecules at the surface. To a first approximation, all orientations of the porphyrin complexes should be reactive at the electrode surface. This is not true for cytochrome b_5, where only those cytochromes with their exposed heme edge facing the electrode surface will be reactive. Estimating that cytochrome b_5 has only a 3.5% active surface area (*11*), the protein still couples to the electrode more poorly by a factor of about 70 times.

The redox center of cytochrome b_5 is able to approach the electrode surface to approximately the same distance as the porphyrin complexes as shown in Figure 5. The significant decrease in the electronic coupling between the porphyrin complexes and cytochrome b_5 is an unexpected result. The major remaining difference between the protein and the porphyrin complexes is the orientation of the heme upon contact with the electrode. It appears this heme orientation plays a significant role in determining the electronic coupling.

Qualitatively, the hypothesis that the heme orientation plays a significant role in controlling its electronic coupling to the electrode surface is supported by a comparison of the electronic coupling between the porphyrin complexes. As the size of the axial ligands increases from *N*-methylimidazole to pyridyl to 4-phenylpyridyl, the electronic coupling

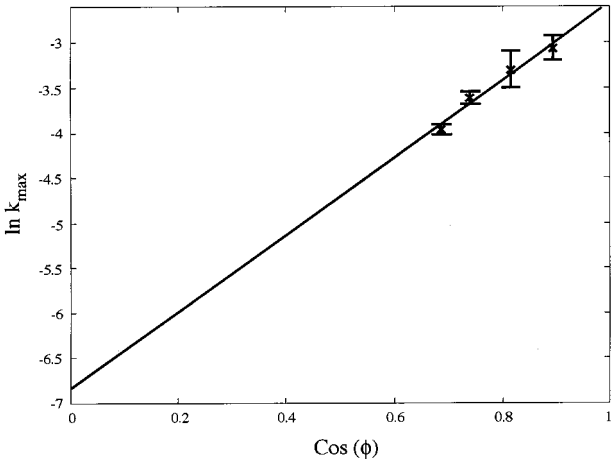

FIGURE 6: Graph of the natural logarithm of the electronic coupling as a function of the cosine of the angle with respect to the electrode surface. The best fit line is displayed to better illustrate linearity.

term, k_{max} values are observed to decrease. Note, given the systematic increase in the electronic coupling with decreasing size of the axial ligand and the virtual identity in reorganization energy of these complexes (see Table 2), it would appear that the known differences in the electronic structure of imidazole and pyridine complexes (*16*, *17*) do not play a major role in the kinetic facility of electron transfer.

The increase in size of the axial ligands will result in small increases in the Fe-electrode surface distance at closest approach along with a concomitant increase in the angle of the porphyrin plane with respect to the electrode surface. If the dominant electronic coupling between the heme and electrode surface is via the parallel overlap of heme and the electrode surface, the rotation of the heme by an angle ϕ away from a parallel orientation could explain the differences in the electronic coupling of these heme models and cytochrome b_5. If we assume the angular dependence of the electronic coupling scales as the projected area of the heme on the electrode surface, then a plot of the $\ln(k_{max})$ versus the $\cos(\phi)$ should be linear and allow an extrapolation to the normal heme orientation of cytochrome b_5 as see in Figure 6. For a heme-to-electrode distance of 7.1 Å calculated for both cytochrome b_5 and the 4-methylpyridyl porphyrin complex, this simple overlap model predicts the heme to be more poorly electronically coupled by a factor of 35. Given the simplicity of this analysis and the limited data, the agreement between this calculated decrease in the electronic coupling of the cytochrome b_5 and the observed factor of 70 is remarkable.

An alternate explanation for the decrease in the electronic coupling of the porphyrin complexes with increasing size

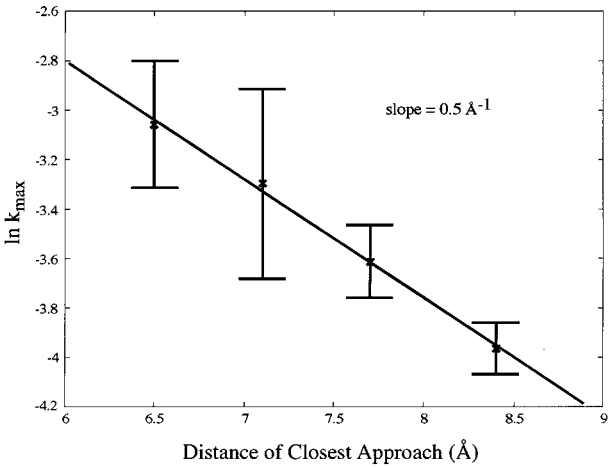

FIGURE 7: Graph of the natural logarithm of the electronic coupling as a function of the distance of closest approach of the redox center for the protein model compounds to the electrode surface. The best fit line is displayed to better illustrate linearity.

of the axial ligands is a simple distance dependence of the electronic coupling between the complex and the electrode surface. A plot of the ln(k_{max}) versus the distance of closest approach is given in Figure 7. Using the correlation from the best fit line in this graph, a tunneling coefficient of 0.5 Å^{-1} is calculated for the porphyrin system. This tunneling coefficient is consistent with other determinations of the distance dependence of electronic coupling for organic systems (*1*, *6*). However, such a simple distance dependence would not predict the significant decrease in the electronic coupling observed for cytochrome b_5 compared to the porphyrin models.

CONCLUSIONS

The reorganization energies of the iron porphyrin complexes are considerably higher than that of the cytochrome b_5. This is expected by the Marcus theory prediction based on the size of the redox species, which are attributed to significant differences in the outer-sphere reorganization energy. The outer-sphere reorganization energy is minimized as the solvent dielectric constant is lowered, revealing the inner-sphere component to the reorganization energy by extrapolation. The protein matrix appears to mimic the limiting behavior of a low dielectric solvent. Major differences in the electronic coupling of the heme model compounds and the cytochromes may be related to differences in the angular orientation of the heme relative to the electrode surface.

REFERENCES

1. Marcus, R. A., and Sutin, N. (1985) *Biochim. Biophys. Acta 811*, 265−322.
2. Marcus, R. A. (1964) *Annu. Rev. Phys. Chem. 15*, 155−197.
3. Muegge, I., Qi, P. X., Wand, A. J., Chu, Z. T., and Warshel, A. (1997) *J. Phys. Chem. B 101*, 825−836.
4. Basu, B., Kitao, A., Kuki, A., and Go, N.(1998) *J. Phys. Chem. B 102*, 2076−2084.
5. Zhou, H.-X. (1994) *J. Am. Chem. Soc. 116*, 10362−10375.
6. Friesner, R. A. (1994) *Structure 2*, 339−343.
7. Beratan, D. N., Onuchic, J. N., Winkler, J. R., and Gray, H. B. (1992) *Science 238*, 1740−1755.
8. McLendon, G(1988) *Acc. Chem. Res. 21*, 160−167.
9. Terrettaz, S., Cheng, J., Miller, C. J., and Guiles, R. D. (1996) *J. Am. Chem. Soc. 118*, 7857−7858.
10. Sarma, S., DiGate, R. J., Goodin, D. B., Miller, C. J., and Guiles, R. D. (1997) *Biochemistry 36*, 5688−5668.
11. Cheng, J., Terrettaz, S., Blankman, J. I.; Miller, C. J., Dangi, B., and Guiles, R. D. (1997) *Isr. J. Chem. 37*, 259−266.
12. Weaver, M. J. (1980) *J. Phys. Chem. 84*, 568−576.
13. Miller, C. J. (1995) Heterogeneous electron-transfer kinetics at metallic electrodes. in *Physical Electrochemistry, Principles, Methods and Applications* (Rubinstein, I., Ed.) pp 27−79, Marcel-Dekker, New York.
14. Becka, A. M., and Miller, C. J. (1992) *J. Phys. Chem. 96*, 2657−2668.
15. Rees, D. K. (1996) *Insulated Electrode Voltammetry in Mixed Aqueous/Non-Aqueous Solvents*, p 66, M.S. Thesis, University of Maryland, College Park.
16. Nesset, M. J. M., Shokhirev, N. V., Enemark, P. D., Jacobson, S. E., and Walker, F. A. (1996) *Inorg. Chem. 35*, 5188−5200.
17. Safo, M. K., Gupta, G. P., Watson, C. T., Simonis, U., Walker, F. A., and Scheidt, W. R. (1992) *J. Am. Chem. Soc. 114*, 7066−7075.
18. Walker, F. A., Huynh, B. H., Scheidt, W. R., and Osvath, S. R. (1986) *J. Am. Chem. Soc. 108*, 5288−5297.
19. von Bodman, S. B., Shuler, M. A., Jollie, D. R., and Sligar, S. G. (1986) *Proc. Natl. Acad. Sci. U.S.A. 83*, 9433−9447.
20. Sarma, S. P., Banville, D., DiGate, R., and Guiles, R. D. (1996) *J. Biomol. NMR 8*, 171−183.
21. Hoshino, M., Ozawa, K., Seki, H., and Ford, P. C. (1993) *J. Am. Chem. Soc. 115*, 9568−9575.
22. Barley, M. H., Takeuchi, K. J., and Meyer, T. J. (1986) *J. Am. Chem. Soc. 108*, 5876−5885.
23. Fleischer, E. B., Palmer, J. M., Srivastava, T. S., and Chatterjee, A. (1971) *J. Am. Chem. Soc. 93*, 3162−3167.
24. Hehre, W. J., Yu, J., and Klumzinger, P. E. (1997) *A Guide to Molecular Mechanics and Molecular Orbital Calculations in SPARTAN*, Wavefunction, Inc., Irvine.
25. Inniss, D., Soltis, S. M., and Strouse, C. E. (1988) *J. Am. Chem. Soc. 110*, 5644−5650.
26. Higgins, T. B., Safo, M. K., Scheidt, W. R. (1990) *Inorg. Chim. Acta 178*, 261−269.
27. Collins, D. M., Countryman, R., and Hoard, J. L. (1972) *J. Am. Chem. Soc. 94*, 2066−2072.
28. Scheidt, W. R., Geiger, D. K., and Haller, K. J. (1982) *J. Am. Chem. Soc. 104*, 495−499.
29. Terrettaz, S., Becka, A. M., Traub, M. J., Fettinger, J. C., and Miller, C. J. (1995) *J. Phys. Chem. 99*, 11216−11224.
30. Becka, A. M., and Miller, C. J. (1993) *J. Phys. Chem. 97*, 6233−6239.
31. Marcus, R. A. (1965) *J. Chem. Phys. 43*, 679−701.
32. Nakamura, H. (1996) *Q. Rev. Biophys. 29*, 1−90.
33. Freeman, F., Lee, S., and Hehre, W. J. (1998) *J. Comput. Chem. 19*, 1064.

BI0007324